Stereoselective Formation of (Aminoalkyl)platinum Complexes from Imines

Cliff R. Baar, Lee P. Carbray, Michael C. Jennings, and Richard J. Puddephatt*

Department of Chemistry, The University of Western Ontario, London, Ontario, Canada N6A 5B7

Jagadese J. Vittal

Department of Chemistry, The National University of Singapore, 3 Science Drive 3, Singapore 117543

Received September 13, 2000

Reaction of $[PtMe_2(\mu\text{-}SMe_2)]_2$ with *cis*-1,2-$C_6H_{10}(N{=}CH\text{-}2\text{-}C_5H_4N)_2$ (**1**) and *cis*-1,2-$C_6H_{10}(N{=}CH\text{-}2\text{-}C_9H_6N)_2$ (**2**) gives the complexes $[PtMe_2\{cis\text{-}1,2\text{-}C_6H_{10}(N{=}CH\text{-}2\text{-}C_5H_4N)_2\}]$ (**3**) and $[PtMe_2\{cis\text{-}1,2\text{-}C_6H_{10}(N{=}CH\text{-}2\text{-}C_9H_6N)_2\}]$ (**4**), respectively (C_5H_4N = pyridyl; C_9H_6N = quinolyl), in which the ligand is bidentate such that each complex is chiral and contains a free imine substituent. Complexes **3** and **4** react with protic acids, HCl and CF_3CO_2H, to form (aminoalkyl)platinum(IV) products that contain a new asymmetric carbon center, often with very high stereoselectivity. In these products the complex ligand may act as a tridentate N,N,C donor or, in complexes containing an azaplatinacyclobutane ring, as a tetradentate N,N,N,C donor. The absolute configurations of five (aminoalkyl)platinum(IV) products were determined by X-ray crystal structure determinations and gave a benchmark such that the stereochemistries of other complexes could be assigned by NMR. It is suggested that the reactions occur by protonation at the free imine nitrogen to give an iminium ion, and the carbocation then adds to the adjacent platinum(II) center. The initially formed products may rearrange by mechanisms involving reversible ligand dissociation from platinum(IV) or deprotonation of the aminoalkyl group.

Introduction

The organometallic chemistry of alkenes and imines can be similar or very different.[1] For example, the insertion of alkenes into metal−carbon bonds has been widely applied in late-transition-metal-catalyzed polymerization reactions but, though insertion of an imine into a metal−carbon bond has been reported, polymerization of imines is often inhibited by the formation of stable, cyclic amidoalkylmetal complexes.[2,3] Transition-metal complexes have also been used as catalysts in the asymmetric hydrogenation of both imines and alkenes.[4] With imines, a key step in the catalytic cycle may involve an amido intermediate which is formed by migratory insertion of the imine into a metal−hydrogen bond.[5] Iminium salts, such as the N,N-dialkyl substituted cations $Me_2NCH_2^+$,[6] coordinate to some transition metals through the C−N double bond (η^2-C,N).[7] There are also reports, including examples with platinum(0), in which coordination of the iminium ion occurs through the electrophilic carbon atom (η^1-C), a reaction that is considered an oxidative addition.[8] The products of iminium ion coordination have shown interesting reactivity toward insertion and reductive coupling reac-

(1) (a) Collman, J. P.; Hegedus, L. S.; Norton, J. R.; Finke, R. G. *Principles and Applications of Organotransition Metal Chemistry*; University Science Books: Mill Valley, CA, 1987. (b) Parshall, G. W.; Ittel, S. D. *Homogeneous Catalysis; The Applications and Chemistry of Catalysis by Soluble Transition Metal Complexes*; Wiley: New York, 1980. (c) Yamamoto, A. *J. Chem. Soc., Dalton Trans.* **1999**, 1027.

(2) (a) Brookhart, M.; Rix, F. C.; DeSimone, J. C.; Barborak, J. C. *J. Am. Chem. Soc.* **1992**, *114*, 5895. (b) Rix, F. C.; Brookhart, M. *J. Am. Chem. Soc.* **1995**, *117*, 1137. (c) Johnson, L. K.; Killian, C. M.; Brookhart, M. *J. Am. Chem. Soc.* **1995**, *117*, 6414. (d) Johnson, L. K.; Mecking, S.; Brookhart, M. *J. Am. Chem. Soc.* **1996**, *118*, 267. (e) Rix, F. C.; Brookhart, M.; White, P. S. *J. Am. Chem. Soc.* **1996**, *118*, 4746. (f) Killian, C. M.; Johnson, L. K.; Brookhart, M. *Organometallics* **1997**, *16*, 2005. (g) Desjardins, S. Y.; Way, A. A.; Murray, M. C.; Adirim, D.; Baird, M. C. *Organometallics* **1998**, *17*, 2382. (h) Small, B. L.; Brookhart, M.; Bennett, A. M. A. *J. Am. Chem. Soc.* **1998**, *120*, 4049. (i) Britovsek, G. J. P.; Gibson, V. C.; Kimberley, B. S.; Maddox, P. J.; McTavish, S. J.; Solan, G. A.; White, A. J. P.; Williams, D. J. *Chem. Commun.* **1998**, 849. (j) Griffiths, E. A. H.; Britovsek, G. J. P.; Gibson, V. C.; Gould, I. R. *Chem. Commun.* **1999**, 1333. (k) Deng, L.; Margl, P.; Ziegler, T. *J. Am. Chem. Soc.* **1999**, *121*, 6479.

(3) (a) Dghaym, R. D.; Yaccato, K. J.; Arndtsen, B. A. *Organometallics* **1998**, *17*, 4. (b) Kacker, S.; Kim, J. S.; Sen, A. *Angew. Chem., Int. Ed.* **1998**, *37*, 1251.

(4) (a) Landis, C. R.; Halpern, J. *J. Am. Chem. Soc.* **1987**, *109*, 1746. (b) Halpern, J. *J. Am. Chem. Soc.* **1991**, *113*, 589. (c) Burk, M. J.; Feaster, J. E. *J. Am. Chem. Soc.* **1992**, *114*, 7266 and references therein. (d) Burk, M. J.; Feaster, J. E.; Nugent, W. M.; Harlow, R. L. *J. Am. Chem. Soc.* **1993**, *115*, 10125. (e) Bakos, J.; Orosz, A.; Heil, B.; Laghmari, M.; Lhoste, P.; Sinou, D. *J. Chem. Soc., Chem. Commun.* **1991**, 1684. (f) Spindler, F.; Pugin, B.; Blaser, H. U. *Angew. Chem., Int. Ed. Engl.* **1990**, *29*, 558. (g) Chan, Y. N. C.; Osborn, J. A. *J. Am. Chem. Soc.* **1990**, *112*, 9400. (h) Willoughby, C. A.; Buchwald, S. L. *J. Am. Chem. Soc.* **1994**, *116*, 8952. (i) Willoughby, C. A.; Buchwald, S. L. *J. Am. Chem. Soc.* **1994**, *116*, 11703. (j) Ringwald, M.; Stürmer, R.; Brintzinger, H. H. *J. Am. Chem. Soc.* **1999**, *121*, 1524.

(5) Becalski, A. G.; Cullen, W. R.; Fryzuk, M. D.; James, B. R.; Kang, G.-J.; Rettig, S. J. *Inorg. Chem.* **1991**, *30*, 5002.

(6) Hellmann, H.; Opitz, G. α-*Aminoalkylation*; Verlag Chemie: Weinheim, Germany, 1960; p 1.

(7) (a) Mason, R.; Rucci, G. *J. Chem. Soc., Chem. Commun.* **1971**, 1132. (b) Fong, C. W.; Wilkinson, G. *J. Chem. Soc., Dalton Trans.* **1975**, 1100.

(8) (a) Sepelak, D. J.; Pierpont, C. G.; Barefield, E. K.; Budz, J. T.; Poffenberger, C. A. *J. Am. Chem. Soc.* **1976**, *98*, 6178. (b) Barefield, E. K.; Sepelak, D. J. *J. Am. Chem. Soc.* **1979**, *101*, 6542.

10.1021/om0007769 CCC: $20.00
Publication on Web 12/21/2000

Chart 1

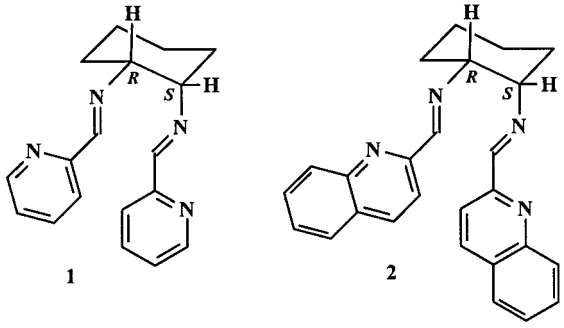

tions,[9] and their transformation into alkylidenes is possible with some transition-metal complexes.[10]

The bis(bidentate) ligand *cis*-1,2-C_6H_{10}(N=CH-2-$C_5H_4N)_2$ (**1**, C_5H_4N = pyridyl; Chart 1), derived from *cis*-1,2-diaminocyclohexane, is a useful supporting ligand for the synthesis of binuclear dimethylplatinum(II) complexes, which react with acids to give electrophilic diplatinum(II) complexes by selective methylplatinum bond cleavage.[11] This paper reports the synthesis and reactivity of the related mononuclear dimethylplatinum(II) complexes, in which one pyridyl and one imine nitrogen of the ligand are not coordinated, including complexes of the similar quinolyl ligand **2** (Chart 1). The dimethylplatinum(II) complexes react with a protic acid in an unusual way to form (aminoalkyl)metal complexes, containing a new metal−carbon bond, and the complexes can be formed with high stereoselectivity. Mechanistically, the reaction is suggested to involve initial protonation of the nitrogen atom of the free imine substituent followed by oxidative addition of the transient iminium intermediate to platinum(II), as illustrated in eq 1. We note that, since many natural

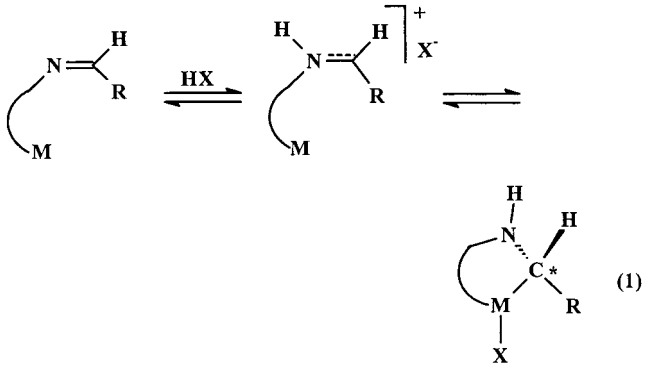

products and pharmaceuticals contain chiral aminoalkyl groups, asymmetric (aminoalkyl)metal complexes are potentially useful synthetic precursors. A part of this work has already been reported as a communication,[12a] and the related chemistry of achiral ligands has also been reported.[12b]

(9) (a) Barefield, E. K.; Carrier, A. M.; Sepelak, D. J.; Van Derveer, D. G. *Organometallics* **1982**, *1*, 103. (b) Barefield, E. K.; Carrier, A. M.; Sepelak, D. J.; Van Derveer, D. G. *Organometallics* **1985**, *4*, 1395.

(10) Beatty, R. P.; Maher, J. M.; Cooper, N. J. *J. Am. Chem. Soc.* **1981**, *103*, 238.

(11) Baar, C. R.; Jennings, M. C.; Puddephatt, R. J.; Muir, K. W. *Organometallics* **1999**, *18*, 4373.

(12) (a) Baar, C. R.; Carbray, L. P.; Jennings, M. C.; Puddephatt, R. J. *J. Am. Chem. Soc.* **2000**, *122*, 176. (b) Baar, C. R.; Jennings, M. C.; Vittal, J. J.; Puddephatt, R. J. *Organometallics* **2000**, *19*, 4150.

Scheme 1

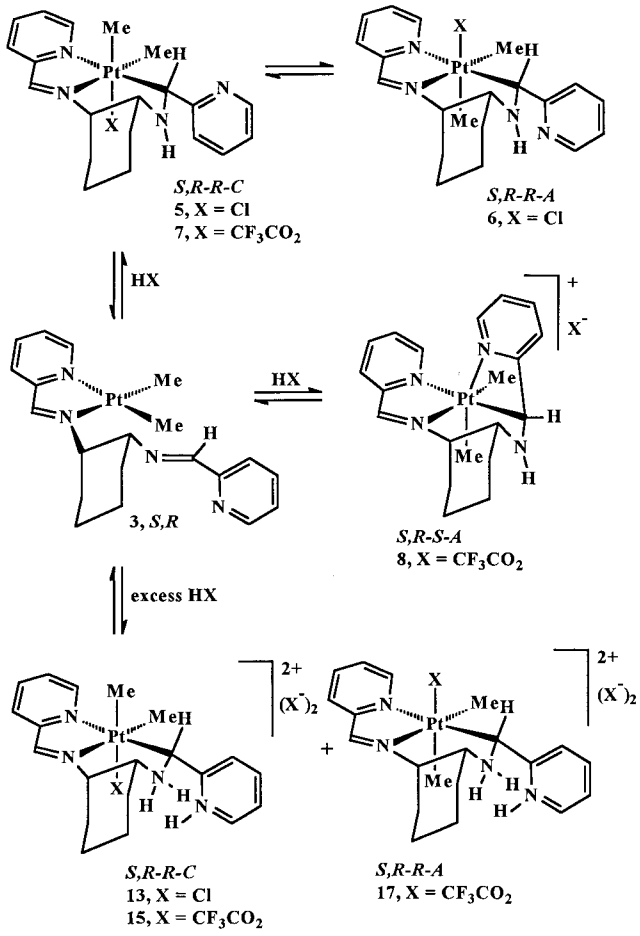

Results

Platinum(II) Complexes. The chemistry of [$PtMe_2$-{*cis*-1,2-C_6H_{10}(*N*=CH-2-C_5H_4N)(N=CH-2-C_5H_4N)}] (**3**) is outlined in Scheme 1. Reaction of [$PtMe_2(\mu$-$SMe_2)]_2$ with 2 equiv of the ligand *cis*-1,2-C_6H_{10}(N=CH-2-$C_5H_4N)_2$ (**1**) gave **3** in high yield. Since complex **3** is formed by the uptake of only one dimethylplatinum(II) unit by the bis(bidentate) ligand, the mirror plane symmetry of the free ligand is lost, and so complex **3** is asymmetric and racemic (only the *S,R* enantiomer is shown in Scheme 1). The structure of **3** was established by its ^{1}H NMR spectrum. Thus, the presence of both free and coordinated imine groups is shown by the observation of equal-intensity singlet resonances at δ 8.18, with no coupling to ^{195}Pt, and at δ 8.91, with satellites due to the coupling ^3J(PtH) = 38 Hz, respectively. In addition, two methylplatinum resonances, each giving typical couplings ^2J(PtH) for a dimethylplatinum(II) complex, are observed.[11,12] The 2-quinolyl derivative [$PtMe_2${*cis*-1,2-C_6H_{10}(*N*=CH-2-C_9H_6N)(N=CH-2-C_9H_6N)}] (**4**) was prepared and characterized similarly. The chemistry of complex **4** is given in Scheme 2.

Reaction of [$PtMe_2${*cis*-1,2-C_6H_{10}(*N*=CH-2-C_5H_4N)-(N=CH-2-C_5H_4N)}] (3) with an Equimolar Amount of HCl. When an NMR tube charged with complex **3** in CD_2Cl_2 was treated with 1 molar equiv of HCl at room temperature, the platinum(II) complex was transformed into a mixture of two platinum(IV) complexes, identified as isomers of [$PtClMe_2${*cis*-1,2-C_6H_{10}(*N*=CH-2-C_5H_4N)-

Scheme 2

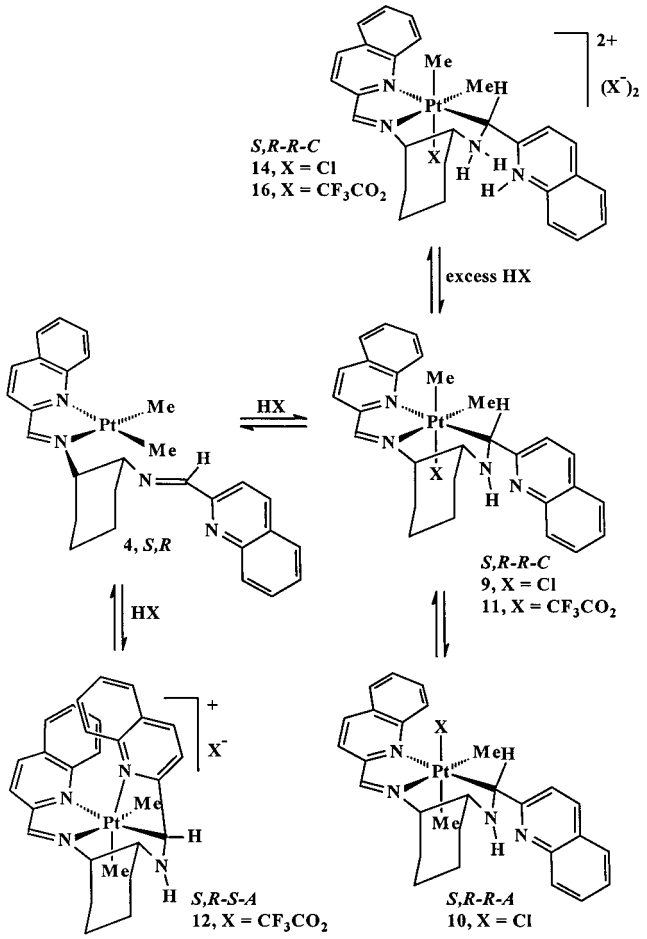

(NHC*H*-2-C_5H_4N)] (**5** and **6**; Scheme 1). The ^{1}H NMR spectrum showed two methylplatinum peaks for each isomer with couplings ^2J(PtMe) in the range expected for methylplatinum(IV) complexes (Table 1).[13] There was no hydride NMR resonance, showing that protonation had not occurred at the platinum(II) center, in contrast to reactions of several other dimethyl(diimine)-platinum(II) complexes.[14] Each isomer gave a single imine resonance, and the observation of the coupling ^3J(PtN=C*H*) showed that the imine was coordinated to platinum. In contrast to **3**, no signal for a free imine group was observed for the isomers **5** and **6**. Instead, new signals were present for the (aminoalkyl)platinum group Pt−C*H*R−NH at δ 4.87 (^2J(Pt−H) = 66 Hz) and at δ 5.92 (^2J(Pt−H) = 140 Hz). The large values of ^2J(Pt−H) (Table 1) show that a new carbon−platinum bond has been formed, though it is not obvious why there is such a large difference in the coupling constants. The presence of aminoalkyl ligands in **5** and **6** was confirmed by X-ray structure determinations for both isomers (see below). When the reaction was monitored by ^{1}H NMR spectroscopy, it was shown that isomer **5** was dominant initially but, after 30 min reaction time, the ratio **5**:**6** reached ca. 1:1 and, after 1 day, complex **6** was by far the dominant product. It is thus clear that **5** is the product of kinetic control but that it then equilibrates slowly with the thermodynamically more stable isomer **6** (Scheme 1). In confirmation, the reaction carried out at −78 °C in CD_2Cl_2 solution gave only isomer **5**, and slow isomerization to **6** was observed only on warming to room temperature.

Single crystals of isomer **5** were obtained by carrying out the reaction of **3** with HCl at low temperature in CH_2Cl_2, followed by slow diffusion of pentane, still at low temperature, to induce crystallization. A view of the structure is given in Figure 1, and selected bond distances and angles are listed in Table 2. Single crystals of isomer **6** were obtained by allowing the products of reaction of **3** with HCl to equilibrate for 1 day at room temperature, followed by slow cooling to −78 °C to induce crystallization. The structure of **6** is shown in Figure 2, with selected bond distances and angles provided in Table 3.

Table 1. ^{1}H NMR Data for 3−17

complex	δ(PtMe) (ppm)	^2J(Pt−H) (Hz)	δ(PtCH-RNH) (ppm)	^2J(Pt−H) (Hz)	δ(N=CH) (ppm)	^3J(Pt−H) (Hz)
3	1.05	86			8.18	38
	1.08	84			8.91	
4	1.32	90			8.36	36
	1.51	84			9.29	
5	0.55	71	4.87	66	9.13	32
	0.65	76				
6	0.37	78	5.92	140	9.17	36
	0.71	72				
7	0.39	80	5.12	64	9.24	38
	0.69	70				
8	0.58	76	4.59	40	9.97	38
	0.94	72				
9	0.51	74	5.05	59	9.36	35
	0.74	72				
10	0.81	79	6.08	138	9.48	35
	1.12	73				
11	0.60	74	5.60	59	9.40	35
	0.79	69				
12	0.86	76	4.98	48	10.28	38
	1.39	71				
13	0.62	64	5.34	70	9.50	33
	1.08	70				
14	0.83	66	5.54	68	9.78	35
	0.98	68				
15	0.68	62	5.50	63	9.30	32
	1.14	72				
16	0.98	63	5.62	62	9.57	34
	1.19	70				
17	0.77	74	6.14	129	9.20	
	0.88	64				

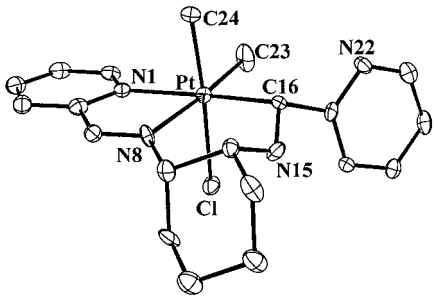

Figure 1. View of the *S,R-R-C* enantiomer of complex **5** (35% probability ellipsoids are shown).

(13) (a) Hill, R. H.; Puddephatt, R. J. *J. Am. Chem. Soc.* **1985**, *107*, 1218. (b) Monaghan, P. K.; Puddephatt, R. J. *Organometallics* **1986**, *5*, 439. (c) Crespo, M.; Puddephatt, R. J. *Organometallics* **1987**, *6*, 2548. (d) Anderson, C. M.; Crespo, M.; Jennings, M. C.; Lough, A. J.; Ferguson, G.; Puddephatt, R. J. *Organometallics* **1991**, *10*, 2672. (e) Anderson, C. M.; Crespo, M.; Ferguson, G.; Lough, A. J.; Puddephatt, R. J. *Organometallics* **1992**, *11*, 1177.

(14) (a) Stahl, S. S.; Labinger, J. A.; Bercaw, J. E. *Angew. Chem., Int. Ed. Engl.* **1998**, *37*, 2181. (b) Hinman, J. G.; Baar, C. R.; Jennings, M. C.; Puddephatt, R. J. *Organometallics* **2000**, *19*, 563. (c) Fekl, U.; Zahl, A.; van Eldik, R. *Organometallics* **1999**, *18*, 4156.

Table 2. Selected Bond Lengths and Angles for Complex 5

(a) Bond Lengths (Å)

Pt−C(23)	2.062(6)	Pt−C(24)	2.066(5)
Pt−C(16)	2.081(6)	Pt−N(8)	2.146(5)
Pt−N(1)	2.187(5)	Pt−Cl	2.4792(14)
N(1)−C(2)	1.333(8)	N(1)−C(6)	1.350(8)
C(7)−N(8)	1.261(7)	N(15)−C(16)	1.451(7)

(b) Bond Angles (deg)

C(23)−Pt−C(24)	88.4(3)	C(23)−Pt−C(16)	91.4(3)
C(24)−Pt−C(16)	88.1(3)	C(23)−Pt−N(8)	173.9(2)
C(24)−Pt−N(8)	90.7(2)	C(16)−Pt−N(8)	94.6(2)
C(23)−Pt−N(1)	97.6(3)	C(24)−Pt−N(1)	89.1(2)
C(16)−Pt−N(1)	170.5(2)	N(8)−Pt−N(1)	76.4(2)
C(23)−Pt−Cl	92.6(2)	C(24)−Pt−Cl	175.92(19)
C(16)−Pt−Cl	95.77(18)	N(8)−Pt−Cl	87.82(14)
N(1)−Pt−Cl	86.89(13)	N(8)−C(7)−C(6)	119.5(7)
C(7)−N(8)−C(9)	119.5(6)	C(7)−N(8)−Pt	115.4(5)
C(9)−N(8)−Pt	125.1(4)	C(14)−N(15)−C(16)	118.7(5)
N(15)−C(16)−C(17)	108.3(5)	N(15)−C(16)−Pt	111.1(4)
C(17)−C(16)−Pt	115.8(4)		

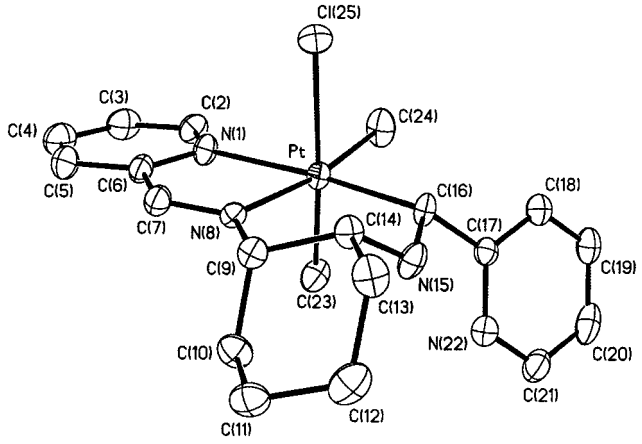

Figure 2. View of the *S,R-R-A* enantiomer of complex **6** (35% probability ellipsoids are shown).

Each complex **5** and **6** contains an octahedral platinum(IV) center containing new bonds to a chloride ligand and to an aminoalkyl group that is formed by protonation/metalation of the free imine substituent in **3**. The aminoalkyl group then becomes part of a meridional N,N,C-tridentate ligand and contains a new asymmetric carbon atom (C(16) in Figures 1 and 2). Within the aminoalkyl group, the bond lengths N(15)−C(16) = 1.451(7) Å in **5** and N(15)−C(16) = 1.455(7) Å in **6** are in the range expected for nitrogen−carbon single bonds. Since the major axis of the octahedron is defined by the Cl−Pt−C(24) vector in Figure 1 and the Cl−Pt−C(23) vector in Figure 2, the free pyridyl ligand is in an equatorial position on the asymmetric carbon atom C(16) for each complex **5** and **6**. The (aminoalkyl)-metal bond lengths, Pt−C(16), are effectively equal in **5** and **6** and slightly longer than the methylplatinum bonds, Pt−C(23) and Pt−C(24) (Figures 1 and 2). For example, in complex **5**, Pt−C(16) = 2.081(6) Å vs Pt−C(23) = 2.062(6) Å and Pt−C(24) = 2.066(5) Å (Table 2). In the structure of complex **5**, there is a water molecule that bridges between two molecules of **5** by hydrogen bonding to the free 2-pyridyl nitrogen atom, N(22), of one molecule and to the chloride ligand of a second molecule. This H-bonding arrangement orients N(22) in a direction *syn* to a methylplatinum(IV) group and *anti* to the chloride ligand (Figure 1). In the structure of complex **6** (Figure 2), the free 2-pyridyl

Table 3. Selected Bond Lengths and Angles for Complex 6

(a) Bond Lengths (Å)

Pt−C(24)	2.045(6)	Pt−C(23)	2.051(7)
Pt−C(16)	2.088(5)	Pt−N(8)	2.129(4)
Pt−N(1)	2.191(5)	Pt−Cl(25)	2.5069(15)
N(1)−C(2)	1.325(8)	N(1)−C(6)	1.361(8)
C(6)−C(7)	1.459(8)	C(7)−N(8)	1.268(7)
N(8)−C(9)	1.472(7)	C(14)−N(15)	1.455(7)
N(15)−C(16)	1.455(7)	C(16)−C(17)	1.521(7)
C(17)−N(22)	1.335(7)		

(b) Bond Angles (deg)

C(24)−Pt−C(23)	89.8(3)	C(24)−Pt−C(16)	91.6(3)
C(23)−Pt−C(16)	92.5(2)	C(24)−Pt−N(8)	171.4(2)
C(23)−Pt−N(8)	94.8(2)	C(16)−Pt−N(8)	95.46(19)
C(24)−Pt−N(1)	96.5(2)	C(23)−Pt−N(1)	87.1(2)
C(16)−Pt−N(1)	171.9(2)	N(8)−Pt−N(1)	76.55(18)
C(24)−Pt−Cl(25)	90.6(2)	C(23)−Pt−Cl(25)	177.02(17)
C(16)−Pt−Cl(25)	90.40(15)	N(8)−Pt−Cl(25)	84.40(11)
N(1)−Pt−Cl(25)	89.92(12)	N(8)−C(7)−C(6)	119.7(5)
C(7)−N(8)−C(9)	118.1(4)	C(7)−N(8)−Pt	115.6(4)
C(9)−N(8)−Pt	126.0(3)	C(14)−N(15)−C(16)	119.1(4)
N(15)−C(16)−C(17)	108.2(4)	N(15)−C(16)−Pt	113.6(4)
C(17)−C(16)−Pt	116.6(4)		

nitrogen atom, N(22), is rotated compared to **5** so that it is again *syn* to a methylplatinum(IV) group and *anti* to the chloride ligand. In this case, N(22) is hydrogen-bonded to a series of water molecules.

The above structural data show that the platinum−carbon distances for the aminoalkyl groups in **5** and **6** are very similar, and so the large difference in the corresponding (aminoalkyl)platinum(IV) coupling constants ^2J(PtH) (Table 1) cannot be correlated to the Pt−C distances. Instead, the large difference is attributed to the conformation of the aminoalkyl bond C(16)−H, which is axially located in both **5** and **6** but lies parallel to a Pt−Me bond in complex **5** and to a Pt−Cl bond in complex **6**.[15]

Figure 1 shows that the absolute configuration of complex **5** is *S,R-R-C*,[16] while Figure 2 shows that the absolute configuration of complex **6** is *S,R-R-A*. Hence, the isomerization of **5** to **6** must involve a change in the absolute configuration at the asymmetric platinum(IV) center and not the chirality at the aminoalkyl carbon atom. The platinum(IV) center can change from *C* to *A* by dissociation of the chloride ligand, migration of the methyl groups, and recoordination of the chloride ligand on the *opposite* diastereotopic face. Although this type of equilibrium was proposed recently for related organoplatinum(IV) complexes, only one isomer was characterized crystallographically in that case.[17]

These results demonstrate that the formation of the (aminoalkyl)platinum(IV) bond occurs with very high stereoselectivity (>99%) at the aminoalkyl carbon atom, since only two complexes, **5** and **6**, were observed by ^{1}H NMR spectroscopy. The enantiomer *S,R* of **3** gives only *S,R-R-C* for **5** and *S,R-R-A* for **6** (Figures 1 and 2), and

(15) It is not obvious why this difference causes such a large difference in *J*(Pt−H) values, but the empirical correlation is strong.

(16) In the descriptor *S,R-R-C*, the first two letters define chirality at the two cyclohexyl carbons, the third defines chirality at the aminoalkyl carbon, and the fourth defines the chirality at platinum (*A* = anticlockwise, *C* = clockwise). Because the complex **3** is actually racemic, each product is also racemic. Block, B. P.; Powell, W. H.; Fernelius, W. C. *Inorganic Chemical Nomenclature: Principles and Practice*; American Chemical Society: Washington, DC, 1990; Chapter 16.

(17) Baar, C. R.; Jenkins, H. A.; Vittal, J. J.; Yap, G. P. A.; Puddephatt, R. J. *Organometallics* **1998**, *17*, 2805.

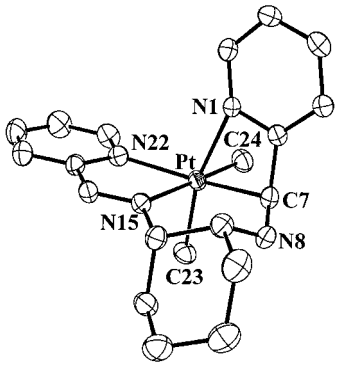

Figure 3. View of the *S,R-S-A* enantiomer of complex **8** (35% probability ellipsoids are shown).

Table 4. Selected Bond Lengths and Angles for 8

	(a) Bond Lengths (Å)		
Pt−C(23)	2.041(4)	Pt−C(24)	2.059(4)
Pt−C(7)	2.070(4)	Pt−N(15)	2.123(3)
Pt−N(1)	2.157(3)	Pt−N(22)	2.209(3)
N(1)−C(2)	1.341(5)	N(1)−C(6)	1.347(5)
C(7)−N(8)	1.418(5)	N(8)−C(9)	1.454(5)
N(15)−C(16)	1.279(5)		
	(b) Bond Angles (deg)		
C(23)−Pt−C(24)	88.78(17)	C(23)−Pt−C(7)	100.12(17)
C(24)−Pt−C(7)	90.34(17)	C(23)−Pt−N(15)	89.85(14)
C(24)−Pt−N(15)	176.54(14)	C(7)−Pt−N(15)	93.03(14)
C(23)−Pt−N(1)	165.70(15)	C(24)−Pt−N(1)	87.40(15)
C(7)−Pt−N(1)	66.15(14)	N(15)−Pt−N(1)	94.68(11)
C(23)−Pt−N(22)	88.42(16)	C(24)−Pt−N(22)	100.34(15)
C(7)−Pt−N(22)	166.51(14)	N(15)−Pt−N(22)	76.44(12)
N(1)−Pt−N(22)	105.82(13)	C(6)−N(1)−Pt	93.7(3)
N(8)−C(7)−C(6)	113.1(3)	N(8)−C(7)−Pt	117.0(3)
C(6)−C(7)−Pt	92.5(2)	C(7)−N(8)−C(9)	118.9(3)
C(16)−N(15)−C(14)	118.6(3)	C(16)−N(15)−Pt	115.8(3)
C(14)−N(15)−Pt	125.3(2)	N(15)−C(16)−C(17)	119.8(3)

the aminoalkyl carbon atom has the *R* configuration in both isomers.

Reaction of [PtMe$_2${*cis*-1,2-C$_6$H$_{10}$(*N*=CH-2-C$_5$H$_4$*N*)-(N=CH-2-C$_5$H$_4$N)}] (3) with 1 Molar Equiv of CF$_3$CO$_2$H. When the protonation of **3** was carried out with 1 molar equiv of CF_3CO_2H in CD_2Cl_2 solution, the major product was [PtMe$_2${*cis*-1,2-C$_6$H$_{10}$(*N*=CH-2-C$_5$H$_4$*N*)(NH-*C*H-2-C$_5$H$_4$*N*)}][CF$_3$CO$_2$] (**8**), formed as a single diastereomer (Scheme 1). The ^{1}H NMR spectrum contained two methylplatinum(IV) peaks and a new resonance at δ 4.59 (^2J(Pt−H) = 40 Hz), assigned to an (aminoalkyl)platinum(IV) proton within a strained azametallacyclobutane ring (Table 1). A minor species, **7**, was also observed, present in yields of up to 20% as discussed further below.

The stereochemistry of **8** was defined by an X-ray structure determination. A view of the structure is given in Figure 3, and selected bond distances and angles are given in Table 4. The 2-pyridyl group which remained free in complexes **5** and **6** is coordinated to platinum(IV) in **8**, making the ligand tetradentate. Because of the N,N,C,N coordination mode, the (aminoalkyl)platinum bond is part of a strained four-membered azametallacyclobutane ring.[18] The Pt−N(1) bond is relatively long at 2.157(3) Å, but the azametallacyclobutane ring structure still causes a significant distortion of the platinum(IV) complex from octahedral geometry. The angle C(7)−Pt−N(1) = 66.1(1)° is compressed from the ideal of 90° to accommodate the four-membered ring. The formation of a ring structure is possibly due to the *axial* location of the 2-pyridyl fragment (the major axis is defined by the N(1)−Pt−C(23) vector) and the weak competition from the trifluoroacetate ligand and is aided by the chelate effect. The formation of complex **8** occurs with essentially perfect stereoselectivity at both the platinum(IV) and aminoalkyl carbon centers, since no other stereoisomers of **8** were observed by ^{1}H NMR spectroscopy. The formation of the azametallacyclobutane ring, along with the constraints imposed by the N,N,C,N coordination mode, is only possible with the relative chiralities at the aminoalkyl and platinum centers observed in **8** (*S,R-S-A*). It is interesting that the chirality of the aminoalkyl carbon atom C(7) is *opposite* to that observed in either complex **5** or **6**.

When the above reaction was monitored by ^{1}H NMR spectroscopy, a second complex **7** was shown to be present in the early stages of the reaction, but it was converted to the thermodynamically preferred product **8** over a period of 1 h. The stereochemistry proposed for **7** in Scheme 1 is based on its NMR spectrum, since it could not be isolated. The complex is thought to contain coordinated trifluoroacetate based on empirical correlation of the chemical shifts of the imine proton (δ 9.24 for **7**). Thus, for the known complexes with a coordinated ligand X = Cl, CF_3CO_2, the imine resonance occurs at δ 9.13−9.48 while, for the azametallacyclobutane complexes, it occurs in the range δ 9.97−10.28 (Table 1). In addition, the magnitude of the coupling constant, ^2J(Pt−H) = 64 Hz, for the aminoalkyl proton of **7** suggests an orientation similar to that in complex **5**, which has ^2J(Pt−H) = 66 Hz (Table 1). Hence, a tentative structural assignment of complex **7** is as the *S,R-R-C* isomer (Scheme 1). If this is correct, the isomerization of **7** to **8** involves inversion at carbon and, thus, must occur by reversible deprotonation to re-form the parent **3** as shown in Scheme 1.

Reactions of AgO$_2$CCF$_3$ and NaCl with 2-Pyridyl Derivatives. The reaction of a mixture of isomers **5** and **6** (X = Cl) with silver trifluoroacetate gave a second route to complex **8** (X = CF_3CO_2). Since the stereochemistry of the aminoalkyl carbon is *opposite* in complex **8**, this reaction must occur with inversion at the aminoalkyl carbon atom. The mechanism of this reaction probably involves abstraction of a chloride ligand from **5** or **6** to generate a five-coordinate cation, followed by reversible loss of a proton from the cationic intermediate to regenerate complex **3**. Finally, protonation at the *opposite* face of the free imine group in **3** occurs to give a second five-coordinate intermediate in which the pyridyl ligand is *axial* and so can coordinate to platinum to give complex **8**. Consistent with this conclusion, reaction of **8** with NaCl regenerated a mixture of isomers **5** and **6**, and once again inversion at the aminoalkyl carbon center is required. The reaction is thus shown to be fully reversible.

(18) Aminoalkyl complexes containing MCCN rings (M = Pd, Pt) can be prepared by reaction of an amide with a metal−alkene complex: (a) Zhang, L.; Zetterberg, K. *Organometallics* **1991**, *10*, 3806. (b) Arnek, R.; Zetterberg, K. *Organometallics* **1987**, *6*, 1230. (c) Jennings, P. W.; Johnson, L. L. *Chem. Rev.* **1994**, *94*, 2241. (d) Mitchenko, S. A.; Zamashchikov, V. V.; Slinkin, S. M. *Russ. J. Gen. Chem. (Engl. Transl.)* **1993**, *63*, 667. (e) Zamashchikov, V. V.; Mitchenko, S. A.; Slinkin, S. M. *Russ. Chem. Bull. (Engl. Transl.)* **1994**, *43*, 478.

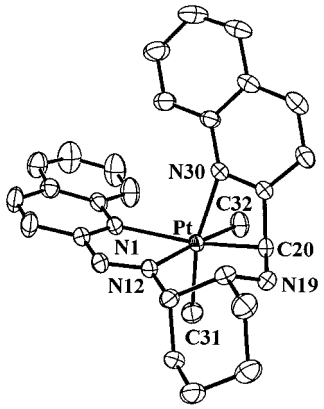

Figure 4. View of the *S,R-S-A* enantiomer of complex **12** (35% probability ellipsoids are shown).

Reaction of [PtMe$_2${*cis*-1,2-C$_6$H$_{10}$(*N*=CH-2-C$_9$H$_6$*N*)-(N=CH-2-C$_9$H$_6$N)}] (4) with 1 Molar Equiv of HCl or CF$_3$CO$_2$H. The reactions of complex **4** with 1 molar equiv of HCl or CF_3CO_2H are similar to those of **3**, as outlined in Scheme 2, but with significant differences arising from the greater bulk of the 2-quinolyl over the 2-pyridyl group.

The reaction of **4** with HCl was monitored by ^{1}H NMR spectroscopy. At room temperature, the complex [PtClMe$_2${*cis*-1,2-C$_6$H$_{10}$(*N*=CH-2-C$_9$H$_6$*N*)(NH-*C*H-2-C$_9$H$_6$N)}] (**9**) was formed first and could be isolated in pure form. Comparison of the NMR data of complex **9** with those of the structurally characterized complexes **5** and **6** (Table 1) allows its characterization as the *S,R-R-C* isomer, analogous to complex **5** (Figure 1). When **9** was dissolved in CD_2Cl_2, it slowly isomerized to complex **10**, eventually giving an equilibrium mixture after 1−2 days in which the ratio **9**:**10** was close to 1:1. Comparison of the ^{1}H NMR data of **10** with those of the structurally characterized **5** and **6** (Table 1) shows that **10** is the *S,R-R-A* isomer, analogous to **6** (Figure 2). The isomerization of **9** to **10** is much slower than the similar reaction of **5** to give **6**.

The reaction of **4** with CF_3CO_2H in CH_2Cl_2 at room temperature gave the azametallacyclobutane complex [PtMe$_2${*cis*-1,2-C$_6$H$_{10}$(*N*=CH-2-C$_9$H$_6$*N*)(NH*C*H-2-C$_9$H$_6$*N*)}][CF$_3$CO$_2$] (**12**) in essentially quantitative yield (Scheme 2). Monitoring the reaction by ^{1}H NMR in CD_2Cl_2 solution at room temperature showed that a second complex **11** was formed first, but this isomerized quickly to **12**. The ^{1}H NMR data (Table 1) suggest a structure with *S,R-R-C* configuration, analogous to complexes **5** and **7** (Scheme 1) and **9** (Scheme 2). The aminoalkyl ligand in complex **12** was characterized by resonances at δ(PtC*H*) = 4.98 (^2J(Pt−H) = 48 Hz) and at δ(Pt*C*H) = 40.5 (^1J(Pt−C) = 524 Hz) in the ^{1}H and ^{13}C NMR spectra, respectively. A feature of the ^{1}H NMR spectrum is the presence of a sharp doublet at δ 6.32, attributed to an aromatic proton involved in an edge-to-face aromatic interaction.[19]

A view of the structure of complex **12** is shown in Figure 4, and selected bond distances and angles are provided in Table 5. The absolute configuration is *S,R-S-A*, analogous to that observed for complex **8**. As with **8**, the free quinolyl ligand is in an *axial* position and coordinates to the platinum(IV) center as part of an azametallacyclobutane ring. The N(30)−Pt−C(20) angle of 65.5(2)° is distorted from the ideal of 90° to allow for N,N,C,N-tetradentate coordination. It is clear from Figure 4 that the aromatic quinolyl ligands face each other in an edge-to-face orientation, placing the hydrogen atom of C(28) in a highly shielded environment. This edge-to-face arrangement may help stabilize the complex, since significant stabilization from such interactions is established in several aromatic systems, including transition-metal complexes.[19]

Table 5. Selected Bond Lengths and Angles for Complex 12

(a) Bond Lengths (Å)			
Pt−C(31)	2.057(5)	Pt−C(32)	2.075(5)
Pt−C(20)	2.109(4)	Pt−N(12)	2.137(4)
Pt−N(30)	2.163(4)	Pt−N(1)	2.339(4)
N(1)−C(10)	1.336(6)	N(1)−C(2)	1.371(6)
C(11)−N(12)	1.266(6)	N(19)−C(20)	1.402(6)
C(20)−C(21)	1.510(6)	C(21)−N(30)	1.322(6)
C(29)−N(30)	1.367(6)		
(b) Bond Angles (deg)			
C(31)−Pt−C(32)	87.6(3)	C(31)−Pt−C(20)	101.9(2)
C(32)−Pt−C(20)	86.7(2)	C(31)−Pt−N(12)	89.60(19)
C(32)−Pt−N(12)	176.74(19)	C(20)−Pt−N(12)	92.24(16)
C(31)−Pt−N(30)	166.44(19)	C(32)−Pt−N(30)	86.7(2)
C(20)−Pt−N(30)	65.50(16)	N(12)−Pt−N(30)	95.62(14)
C(31)−Pt−N(1)	91.40(18)	C(32)−Pt−N(1)	106.63(19)
C(20)−Pt−N(1)	161.70(16)	N(12)−Pt−N(1)	75.15(14)
N(30)−Pt−N(1)	102.02(13)	N(12)−C(11)−C(10)	120.3(4)
C(11)−N(12)−C(13)	118.4(4)	C(11)−N(12)−Pt	117.1(3)
C(13)−N(12)−Pt	124.3(3)	C(20)−N(19)−C(18)	120.5(4)
N(19)−C(20)−C(21)	114.9(4)	N(19)−C(20)−Pt	117.0(3)
C(21)−C(20)−Pt	90.9(3)		

Reactions of AgO$_2$CCF$_3$ and NaCl with 2-Quinolyl Derivatives. To confirm the reversibility of Scheme 2, the reaction of **9** with silver trifluoroacetate was carried out. As with the 2-pyridyl analogues, a second route to the azametallacyclobutane complex **12** was obtained. Likewise, the reaction of **12** with NaCl gave a mixture of complexes **9** and **10**.

Reactions of [PtMe$_2${*cis*-1,2-C$_6$H$_{10}$(*N*=CH-2-C$_5$H$_4$*N*)-(N=CH-2-C$_5$H$_4$N)}] (3) and [PtMe$_2${*cis*-1,2-C$_6$H$_{10}$(*N*=CH-2-C$_9$H$_6$*N*)(N=CH-2-C$_9$H$_6$N)}] (4) with Excess Acid. The (aminoalkyl)platinum(IV) complexes are stable in acidic media, and the major products of the reactions of **3** and **4** with excess acid are included in Schemes 1 and 2. The reactions of **3** and **4** with excess HCl gave the triply protonated complexes [PtClMe$_2${*cis*-1,2-C$_6$H$_{10}$(*N*=CH-2-C$_5$H$_4$*N*)(NH$_2$*C*H-2-C$_5$H$_4$NH)}][Cl]$_2$ (**13**) and [PtClMe$_2${*cis*-1,2-C$_6$H$_{10}$(*N*=CH-2-C$_9$H$_6$*N*)(NH$_2$-*C*H-2-C$_9$H$_6$NH)}][Cl]$_2$ (**14**), respectively, and the reactions with excess trifluoroacetic acid gave the corresponding trifluoroacetate derivatives **15** and **16**. The complexes **13** and **14** derived from HCl addition were sparingly soluble in common organic solvents, and they precipitated as they formed. While the trifluoroacetate complex **16** (Scheme 2) was formed as a single isomer, complex **15** was formed along with about 10% of a minor isomer, tentatively identified as **17** from its NMR data (Table 1). Complexes **15** and **17** differ in relative chirality at platinum (Scheme 1). The products derived from excess CF_3CO_2H are more soluble than those from reactions with HCl, but all these complexes are isolated as hygroscopic solids. The formation of these cationic complexes involves protonation of amine and free py-

(19) (a) Nishio, M.; Hirota, M.; Umezawa, Y. *The CH/π Interaction*; Wiley-VCH: New York, 1998. (b) Hunter, C. A. *Chem. Soc. Rev.* **1994**, 101. (c) Hunter, C. A.; Sanders, J. K. M. *J. Am. Chem. Soc.* **1990**, *112*, 5525.

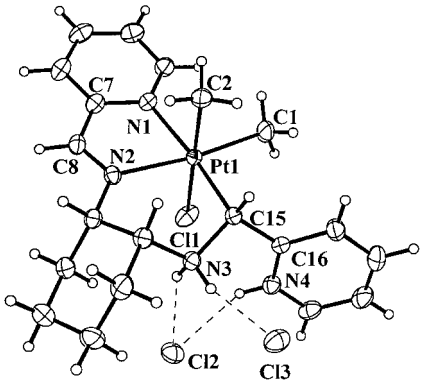

Figure 5. View of the *S,R-R-C* enantiomer of complex **13** (35% probability ellipsoids are shown).

Table 6. Selected Bond Lengths and Angles for Complex 13

(a) Bond Lengths (Å)

Pt(1)−C(1)	2.062(5)	Pt(1)−C(2)	2.072(5)
Pt(1)−C(15)	2.074(5)	Pt(1)−N(1)	2.129(4)
Pt(1)−N(2)	2.147(4)	Pt(1)−Cl(1)	2.4526(13)
C(8)−N(2)	1.267(6)	N(3)−C(15)	1.517(6)

(b) Bond Angles (deg)

C(1)−Pt(1)−C(2)	87.7(3)	C(1)−Pt(1)−C(15)	90.7(2)
C(2)−Pt(1)−C(15)	90.2(2)	C(1)−Pt(1)−N(1)	96.1(2)
C(2)−Pt(1)−N(1)	87.3(2)	C(15)−Pt(1)−N(1)	172.66(17)
C(1)−Pt(1)−N(2)	172.6(2)	C(2)−Pt(1)−N(2)	88.88(19)
C(15)−Pt(1)−N(2)	95.89(16)	N(1)−Pt(1)−N(2)	77.16(16)
C(1)−Pt(1)−Cl(1)	90.1(2)	C(2)−Pt(1)−Cl(1)	176.50(18)
C(15)−Pt(1)−Cl(1)	92.53(13)	N(1)−Pt(1)−Cl(1)	90.20(12)
N(2)−Pt(1)−Cl(1)	92.95(11)	N(2)−C(8)−C(7)	119.4(5)
C(8)−N(2)−C(9)	118.3(4)	C(8)−N(2)−Pt(1)	114.4(3)
C(9)−N(2)−Pt(1)	127.1(3)	C(10)−N(3)−C(15)	114.6(4)
C(16)−C(15)−N(3)	108.9(4)	C(16)−C(15)−Pt(1)	117.6(3)
N(3)−C(15)−Pt(1)	110.4(3)		

ridyl or quinolyl groups, as shown in Schemes 1 and 2.[20] For complexes **15** and **16**, the presence of both free and coordinated trifluoroacetate was supported by the observation of two resonances in the ^{19}F NMR spectrum.[20] For example, the ^{19}F NMR spectrum of **16** had resonances at δ −76.3 and −75.8, assigned to coordinated and free trifluoroacetate, respectively.

The structure of complex **13** was confirmed by an X-ray structure determination. A view of the structure is provided in Figure 5, and selected bond lengths and angles are provided in Table 6. The core structure is very similar to that of complex **5** (compare Figures 1 and 5, *S,R-R-C* configuration in each case). In **13**, extra protons have been added to the aminoalkyl nitrogen, N(3), and to the free 2-pyridyl nitrogen atom compared to **5**. The two protons of the aminoalkyl nitrogen, N(3), are each hydrogen-bonded to a chloride anion Cl(2) and Cl(3), and Cl(2) is also hydrogen-bonded to the pyridinium hydrogen N(4)−H. This bridging arrangement causes N(4) of the free pyridinium center to orient itself *syn* to N(3) in **13**, whereas it was *anti* in complex **5**. There also appears to be weak hydrogen bonding between one N(3)−H proton and the chloride ligand Cl(1) (Figure 5), and this perhaps stabilizes the *S,R-R-C* configuration in the cation.

The presence of intramolecular hydrogen bonding thus appears to favor one configuration at platinum, while the acidic medium prohibits deprotonation back to the parent molecules **3** and **4** (Schemes 1 and 2) and so prevents inversion at carbon. The overall result is that the multiply protonated complexes in general appear to exist as the "kinetic" isomers, first formed by protonation of the parent molecules **3** and **4** (Schemes 1 and 2).

Discussion of Mechanism and Stereochemistry

The observation of kinetically and thermodynamically controlled products in some reactions of **3** and **4** with HCl at ambient temperatures provides insight into the mechanism responsible for the observed stereoselectivity of these reactions. There are four possible diastereomers that can be formed from the metalation of the imine in asymmetric (*S,R*) **3** or **4**: *S,R-R-C* (observed for **5** and **9**), *S,R-R-A* (observed for **6** and **10**), *S,R-S-C* (not observed), and *S,R-S-A* (observed for **8** and **12**). Activation of the imine ligand should initially form a Pt−C bond above or below the square plane of complex **3** or **4**, to give a *fac*-N,N,C-ligated platinum(IV) complex.[21] The proposed facial intermediate was not readily observed and is suggested to rearrange rapidly by migration of the newly formed aminoalkyl ligand to form the meridional isomer. The chloride ligand then adds at the site initially occupied by the aminoalkyl carbon, thus marking the location of platinum−carbon bond formation. Support for formation of a facial intermediate was obtained by carrying out low-temperature reactions with the 2-quinolyl derivative **4** with 1 equiv of CF_3CO_2H, the reaction being monitored by NMR at −78 °C in CD_2Cl_2 solution. After a few minutes, an (aminoalkyl)platinum(IV) species was observed, indicated by a resonance at δ 4.86 (^2J(Pt−H) = 54 Hz) and with methylplatinum(IV) resonances at δ 0.74 (^2J(Pt−H) = 73 Hz) and δ 1.29 (^2J(Pt−H) = 72 Hz). The very similar coupling constants for the methylplatinum ligands supports the presence of a facial intermediate in which the methylplatinum ligands are trans to a pyridyl and imine group, which have similar trans influences.[11,12,17] The ^{1}H NMR spectrum also gives an aromatic proton resonance at δ 6.2, indicating the presence of an edge-to-face orientation of the 2-quinolyl ligands, similar to that observed in the fully characterized complex **12**. As the temperature was increased slowly, the proposed *fac* intermediate isomerized and finally gave complex **12**. The similar reaction of **4** with HCl also gave a shortlived intermediate, that is proposed to have the tridentate N,N,C-bonded ligand in the facial geometry. In the ^{1}H NMR spectrum, the aminoalkyl resonance was at δ 4.70 (^2J(Pt−H) = 50 Hz) and methylplatinum(IV) peaks were at δ 0.69 and 1.23 with identical platinum coupling constants of (^2J(Pt−H) = 71 Hz). The characteristic high-field-shifted aromatic resonance was at δ 6.19. As the temperature was increased, this complex isomerized to give the complex **9** and then, at room temperature, **9** began isomerization to complex **10** (Scheme 2). These proposed facial intermediates were not detected in the corresponding reactions of complex **3**. We propose that the difference arises from the greater steric bulk of the quinolyl group over pyridyl, which hinders the rearrangement reactions.

(20) Single crystals of an achiral analogue of complex **15** have been obtained, and the X-ray crystal structure confirmed the coordination of the trifluoroacetate ligand to the platinum(IV) center.[12b]

(21) A facial intermediate is expected if an S_N2 mechanism operates.[17]

Scheme 3

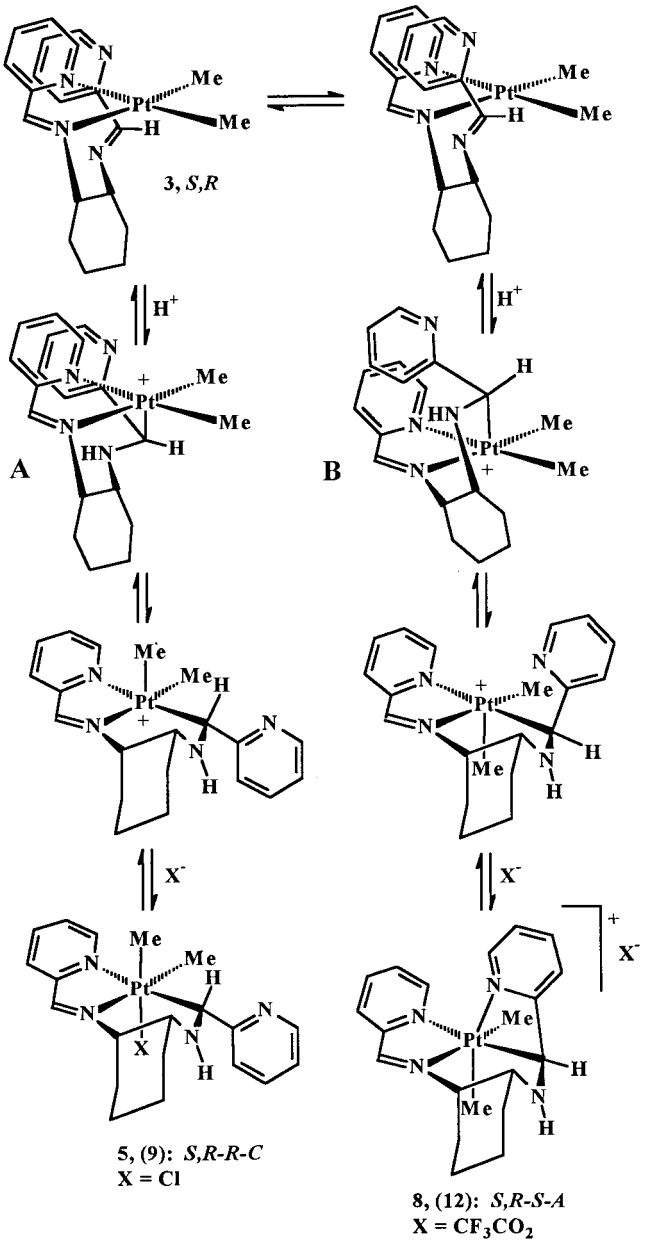

An overall mechanism consistent with these results is shown in Scheme 3, shown for reactions of complex **3** only. Complexes **5** and **9** are formed by protonation/metalation of the imine substituent in a conformation that allows for efficient π-stacking of the aromatic groups and occurs *below* the square plane of **3** and **4** to give a short-lived *fac*-N,N,C tridentate ligand (**A**, Scheme 3). This is followed by aminoalkyl group migration into the meridional plane before coordination of the chloride ligand (X = Cl) to give **5** (*S*,*R*-*R*-*C* configuration) as the kinetically controlled product. To convert **5** to **8**, inversion at the aminoalkyl carbon atom is needed. This must occur by reversal of the above reactions to re-form **3**, followed by protonation at the opposite face of the imine (Scheme 3). In this case metalation occurs *above* the square plane with the imine face chosen to maximize π-overlap between the planar pyridyl or quinolyl fragments (**B**; Scheme 3). Migration of the aminoalkyl group into the meridional plane followed by coordination of the 2-pyridyl group gives complex **8** (*S*,*R*-*S*-*A* configuration). The reactions of the quinolyl derivative **4** can be interpreted similarly, but the rearrangements are all slower, and thus, more intermediates can be detected.

It is clear form these reactions (Schemes 1−3) that the imine substituent in **3** and **4** is more basic than the platinum(II) center and is the preferred site of electrophilic attack, since no dimethylhydridoplatinum(IV) intermediates were observed to be formed.

Experimental Section

General Procedures. All reactions were carried out using standard Schlenk techniques, unless otherwise noted. NMR spectra were recorded using a Varian Gemini spectrometer (^{1}H at 300.10 MHz). Chemical shifts are reported relative to TMS (^{1}H) or $CFCl_3$ (^{19}F). The ^{19}F chemical shifts are referenced to $CFCl_3$ contained in a coaxial insert. IR spectra were recorded as Nujol mulls or thin films in the range 4000−400 cm^{-1} using a Perkin-Elmer 2000 FT-IR instrument. The complex $[PtMe_2(\mu\text{-}SMe_2)]_2$ and the ligands **1** and **2** were prepared by the literature methods.[11,22,23]

***R,S/S,R*-[PtMe$_2$\{*cis*-1,2-C$_6$H$_{10}$(*N*=CH-2-C$_5$H$_4$*N*)(N=CH-2-C$_5$H$_4$N)\}] (3).** To a solution of the ligand *cis*-1,2-C_6H_{10}(N=CH-2-C_5H_4N)$_2$ (**1**; 0.30 g, 1.00 mmol) in diethyl ether (10 mL) was added $[PtMe_2(\mu\text{-}SMe_2)]_2$ (0.27 g, 0.47 mmol). The solution turned red, and in minutes a red precipitate separated. After the mixture was stirred for 24 h, the orange-red precipitate was isolated by filtration and washed with small amounts of diethyl ether (5 × 2 mL) and then pentane (3 × 10 mL). Yield: 0.42 g (86%). Anal. Calcd for $C_{20}H_{26}N_4Pt$: C, 46.4; H, 5.1; N, 10.8. Found: C, 46.3; H, 5.2; N, 10.5. ^{1}H NMR (CD_2Cl_2): δ 1.05 [s, 3H, ^2J(Pt−H) = 86 Hz, PtMe]; 1.08 [s, 3H, ^2J(Pt−H) = 84 Hz, PtMe]; 1.52−2.18 [br m, 7H, Cy]; 2.48 [br m, 1H, Cy]; 4.15 [br s, 1H, NCH]; 4.78 [br d, 1H, NCH]; 7.25 [br t, 1H]; 7.47 [d, 2H]; 7.70 [br t, 1H]; 7.95 [d, 2H]; 8.18 [s, 1H, N=CH]; 8.49 [br d, 1H]; 8.91 [s, 1H, ^3J(Pt−H) = 38 Hz, N=CH]; 9.09 [br d, 1H].

***R,S/S,R*-[PtMe$_2$\{*cis*-1,2-C$_6$H$_{10}$(N=CH-2-C$_9$H$_6$N)(N=CH-2-C$_9$H$_6$N)\}] (4)**, a deep purple powder, was similarly prepared from ligand **2**. Yield: 82%. Anal. Calcd for $C_{28}H_{30}N_4Pt$: C, 54.5; H, 4.9; N, 9.1. Found: C, 54.6; H, 5.2; N, 9.0. ^{1}H NMR (CD_2Cl_2): δ 1.32 [s, 3H, ^2J(Pt−H) = 90 Hz, PtMe]; 1.51 [s, 3H, ^2J(Pt−H) = 84 Hz, PtMe]; 1.55−2.23 [br m, 7H, Cy]; 2.56 [m, 1H, Cy]; 4.26 [br s, 1H, NCH]; 4.91 [m, 1H, NCH]; 7.39 [d, 1H]; 7.48−7.68 [m, 3H]; 7.77−7.88 [m, 4H]; 8.06−8.19 [m, 2H]; 8.36 [s, 1H, N=CN]; 8.38 [d, 1H]: 9.00 [br d, 1H]; 9.29 [d, 1H, ^3J(Pt−H) = 36 Hz, N=CH].

***R,S/S,R*-[PtClMe$_2$\{*cis*-1,2-C$_6$H$_{10}$(*N*=CH-2-C$_5$H$_4$*N*)(NHCH-2-C$_5$H$_4$N)\}] (5 and 6).** To a red suspension of **3** (0.052 g, 0.100 mmol) in diethyl ether (10 mL) was added 1 equiv of HCl, generated in situ by the addition of H_2O (1.8 μL, 0.100 mmol) followed by Me_3SiCl (12.6 μL, 0.100 mmol). The red suspension changed to a yellow-orange solution, and a pale orange precipitate began to separate. After it was stirred for 12 h, the precipitate was isolated by filtration and washed with diethyl ether (3 × 20 mL). NMR showed the orange product was a mixture of compounds **5** and **6**, which are very hygroscopic once isolated. Yield: 0.041 g (67%). Anal. Calcd for $C_{20}H_{33}N_4PtClO_3$: C, 39.5; H, 5.5; N, 9.2. Found: C, 39.6; H, 5.2; N, 9.2. Complexes **5** and **6** were also prepared in CD_2Cl_2 solution by reaction of **3** with 1 molar equiv of HCl. After 30 min of reaction time the ratio is 1:1. ^{1}H NMR (CD_2Cl_2) for **5**: δ 0.55 [s, 3H, ^2J(Pt−H) = 71 Hz, PtMe]; 0.65 [s, 3H, ^2J(Pt−H) = 76 Hz, PtMe]; 3.15 [br s, 1H, NCH]; 3.93 [m, 1H, NCH]; 4.87 [s, 1H, ^2J(Pt−H) = 66 Hz, PtCHR−NH]; 8.40 [m, 1H]; 9.13 [s, 1H, ^3J(Pt−H) = 32 Hz, N=CH]. ^{1}H NMR (CD_2Cl_2) for

(22) Baar, C. R.; Carbray, L. P.; Jennings, M. C.; Puddephatt, R. J. *Organometallics* **2000**, *19*, 2482.
(23) Hill, G. S.; Irwin, M. J.; Levy, C. J.; Rendina, L. M.; Puddephatt, R. J. *Inorg. Synth.* **1998**, *32*, 149.

6: δ 0.37 [s, 3H, ^2J(Pt−H) = 78 Hz, PtMe]; 0.71 [s, 3H, ^2J(Pt−H) = 72 Hz, PtMe]; 1.48−2.10 [m, 8H, Cy]; 3.71 [br s, 1H, NCH]; 3.77 [m, 1H, NCH]; 5.92 [s, 1H, ^2J(Pt−H) = 140 Hz, PtCHR−NH]; 7.12 [m, 2H]; 7.60 [m, 1H]; 7.64 [m, 1H]; 7.92 [d, 1H]; 8.05 [t d, 1H]; 8.48 [d, 1H]; 8.73 [d, 1H]; 9.17 [s, 1H, ^3J(Pt−H) = 36 Hz, N=CH]. ^{13}C NMR (CD_2Cl_2) for **6**: δ −2.5 [^1J(Pt−C) = 757 Hz, PtMe]; 0.2 [^1J(Pt−C) = 745 Hz, PtMe]; 19.5 [CH_2]; 25.3 [CH_2]; 31.4 [CH_2]; 31.8 [CH_2]; 47.8 [^1J(Pt−C) = 611 Hz, PtCHR−NH]; 54.6 [^2J(Pt−C) = 23 Hz, NCH]; 57.5 [^3J(Pt−C) = 16 Hz, NCH]; 120.5 [^3J(Pt−C) = 14 Hz, CH]; 123.6 [^3J(Pt−C) = 16 Hz, CH]; 127.6 [^3J(Pt−C) = 6 Hz, CH]; 128.7 [CH]; 135.0 [CH]; 139.5 [CH]; 147.4 [^2J(Pt−C) = 15 Hz, CH]; 147.7 [CH]; 149.9 [C]; 152.5 [C]; 164.6 [^2J(Pt−C) = 9 Hz, N=CH]. IR (Nujol, cm^{-1}): 724 (w), 754 (w), 784 (w), 1108 (w), 1158 (w), 1232 (w), 1307 (w), 1596 (m), 1621 (m), 2468 (w), 2658 (m), 2718 (m), 3376 (br s).

***R,S/S,R*-[PtMe$_2${*cis*-1,2-C$_6$H$_{10}$(*N*=CH-2-C$_5$H$_4$*N*)(NH*C*H-2-C$_5$H$_4$*N*)}][CF$_3$CO$_2$] (8).** CF_3CO_2H (0.0085 mL, 0.11 mmol) was added to a red solution of **4** (0.058, 0.11 mmol) in CH_2Cl_2 (8 mL), changing the color to yellow. After 1 h the solvent was removed under reduced pressure to give a microcrystalline yellow powder, which was recrystallized from CH_2Cl_2 (1−3 mL) and pentane (10−20 mL) at low temperature. The product is hygroscopic once isolated. Yield: 0.056 g (79%). Anal. Calcd for $C_{22}H_{30}N_4PtO_{3.5}F_3$: C, 40.1; H, 4.6; N, 8.5. Found: C, 40.1; H, 4.4; N, 8.3. ^{1}H NMR (CD_2Cl_2): δ 0.58 [s, 3H, ^2J(Pt−H) = 76 Hz, PtMe]; 0.94 [s, 3H, ^2J(Pt−H) = 72 Hz, PtMe]; 1.22−2.20 [br m, 8H, Cy]; 2.59 [br s, 1H, NCH]; 3.79 [m, 1H, NCH]; 4.59 [s, 1H, ^2J(Pt−H) = 40 Hz, PtCH−NH]; 7.32 [m, 1H]; 7.36 [d, 1H]; 7.75−7.88 [m, 3H]; 8.25 [t d, 1H]; 8.55 [d, 1H]; 8.73 [d, 1H]; 9.97 [s, 1H, ^3J(Pt−H) = 38 Hz, N=CH]. ^{13}C NMR (CD_2Cl_2): δ −10.7 [^1J(Pt−C) = 738 Hz, PtMe]; −3.7 [^1J(Pt−C) = 722 Hz, PtMe]; 19.4 [CH_2]; 25.3 [CH_2]; 31.1 [CH_2]; 31.3 [CH_2]; 34.2 [^1J(Pt−C) = 533 Hz, PtCH−NH]; 51.6 [^2J(Pt−C) = 30 Hz, NCH]; 65.4 [^3J(Pt−C) = 8 Hz, NCH]; 123.6 [^3J(Pt−C) = 43 Hz, CH]; 125.1 [^3J(Pt−C) = 9 Hz, CH]; 128.7 [^3J(Pt−C) = 8 Hz, CH]; 130.6 [CH]; 138.0 [CH]; 140.9 [CH]; 145.5 [^2J(Pt−C) = 8 Hz, CH]; 148.0 [^2J(Pt−C) = 17 Hz, CH]; 153.0 [C]; 168.8 [^2J(Pt−C) = 13 Hz, N=CH]; 172.6 [*ipso*-C]. ^{19}F NMR (CD_2Cl_2): δ −75.6 (s). IR (thin film from CH_2Cl_2): 724 (m), 779 (m), 804 (m), 1013 (m), 1128 (s), 1173 (s), 1208 (s), 1312 (w), 1452 (s), 1477 (s), 1571 (w), 1601 (m), 1691 (s), 2937 (s), 3067 (w), 3316 (br s), 3446 (br s).

***R,S/S,R*-[PtClMe$_2${*cis*-1,2-C$_6$H$_{10}$(*N*=CH-2-C$_9$H$_6$*N*)(NH*C*H-2-C$_9$H$_6$N)}] (9).** HCl (0.73 mmol), generated in situ from H_2O/Me_3SiCl, was added to a cold purple solution of **4** (0.045 g, 0.73 mmol) in CH_2Cl_2 (10 mL) at −78 °C. The color changed to orange. The solution was concentrated at low temperature, followed by pentane addition, which precipitated an orange solid. The product was washed with pentane (3 × 10 mL), warmed to room temperature, and dried extensively under vacuum. The presence of water was confirmed by proton NMR. Yield: 0.041 g (83%). Anal. Calcd for $C_{28}H_{33}N_4OPtCl$: C, 50.0; H, 5.0; N, 8.3. Found: C, 50.4; H, 4.5; N, 8.2. ^{1}H NMR (CD_2Cl_2): δ 0.51 [s, 3H, ^2J(Pt−H) = 74 Hz, PtMe]; 0.74 [s, 3H, ^2J(Pt−H) = 72 Hz, PtMe]; 1.57 [br m, 5H, Cy]; 1.80 [m, 1H, Cy]; 2.08 [m, 1H, Cy]; 2.57 [m, 1H, Cy]; 2.94 [br s, 1H, NH]; 3.22 [br s, 1H, NCH]; 4.26 [m, 1H, NCH]; 5.05 [s, 1H, ^2J(Pt−H) = 59 Hz, PtCHR−NH]; 7.52 [m, 1H]; 7.61−7.79 [m, 4H]; 7.84 [d, 1H]; 7.95 [d, 2H]; 8.22 [br d, 1H]; 8.47 [d, 1H]; 8.58 [d, 2H]; 9.36 [s, 1H, ^3J(Pt−H) = 35 Hz, N=CH].

***R,S/S,R*-[PtMe$_2${*cis*-1,2-C$_6$H$_{10}$(*N*=CH-2-C$_9$H$_6$*N*)(NHCH-2-C$_9$H$_6$*N*)}][CF$_3$CO$_2$] (12)**. To a blue suspension of **4** (0.10 g, 0.17 mmol) in diethyl ether (10 mL) was added 1 equiv of CF_3CO_2H (0.013 mL, 0.17 mmol), turning the solution a dark orange. The solution was stirred for 15 h, and a peach-colored solid precipitated, which was isolated by filtration. The product was then washed with pentane (3 × 10 mL). Yield: 0.92 g (76%). Anal. Calcd for $C_{30}H_{31}N_4PtF_3O_2$: C, 49.3; H, 4.3; N, 7.7. Found: C, 49.3; H, 4.3; N, 7.3. ^{1}H NMR (CD_2Cl_2): δ 0.86 [s, 3H, ^2J(Pt−H) = 76 Hz, PtMe]; 1.39 [s, 3H, ^2J(Pt−H) = 71 Hz, PtMe]; 1.42−2.01 [br m, 8H, Cy]; 2.69 [br s, 1H, NCH]; 3.95 [b, 1H, NCH]; 4.98 [s, 1H, ^2J(Pt−H) = 48 Hz, PtCHR−NH]; 6.32 [d, 1H]; 7.25 [m, 1H]; 7.47 [m, 1H]; 7.51 [d, 1H]; 7.83−7.90 [m, 2H]; 7.96 [m, 1H]; 8.17 [d d, 1H]; 8.32 [d d, 1H]; 8.59 [d, 1H]; 8.73 [d, 1H]; 8.79 [d, 1H]; 10.28 [d, 1H, ^3J(Pt−H) = 38 Hz]. ^{13}C NMR (CD_2Cl_2): δ −10.3 [^1J(Pt−C) = 745 Hz, PtMe]; −1.1 [^1J(Pt−C) = 740 Hz, PtMe]; 19.4 [CH_2]; 25.3 [CH_2]; 30.8 [CH_2]; 31.1 [CH_2]; 40.5 [^1J(Pt−C) = 524 Hz, PtCHRNH]; 51.7 [^2J(Pt−C) = 30.3 Hz, NCH]; 66.7 [NCH]; 120.0 [^3J(Pt−C) = 48 Hz, CH]; 123.9 [^3J(Pt−C) = 9 Hz, CH]; 125.6 [CH]; 127.7 [CH]; 128.2 [CH]; 128.6 [C]; 129.2 [CH]; 129.4 [CH]; 130.1 [CH]; 130.8 [C]; 132.0 [CH]; 133.2 [CH]; 138.9 [CH]; 141.6 [CH]; 143.7 [C]; 148.1 [C]; 153.7 [^2J(Pt−C) = 17 Hz, C]; 171.0 [^2J(Pt−C) = 16 Hz, N=CH]; 172.3 [^2J(Pt−C) = 89 Hz, *ipso*-C]. ^{19}F NMR (CD_2Cl_2): δ −75.4 (s). IR (Nujol, cm^{-1}): 706 (w), 752 (w), 1125 (m), 1157 (m), 1199 (m), 1507 (w), 1594 (w), 1682 (s), 2608 (w), 2663 (w), 2727 (w), 3188 (w), 3409 (br s).

***R,S/S,R*-[PtClMe$_2${*cis*-1,2-C$_6$H$_{10}$(*N*=CH-2-C$_5$H$_4$*N*)(NH$_2$*C*H-2-C$_5$H$_4$NH)}][Cl]$_2$ (13).** HCl (0.173 mmol, generated in situ with 3.1 μL of H_2O and 22.1 μL of Me_3SiCl) was added to a stirred solution of **3** (0.03 g, 0.058 mmol) in CH_2Cl_2 (10 mL), changing the color from red to yellow. Within minutes a pale yellow precipitate started to separate. After the mixture was stirred for 15 h, the supernatant was removed via cannula and the product washed with CH_2Cl_2 (3 × 8 mL) and dried under reduced pressure. Yield: 75%. Anal. Calcd for $C_{20}H_{31}N_4PtCl_3O$: C, 37.3; H, 4.8; N, 8.7. Found: C, 36.8; H, 4.8; N, 8.5. ^{1}H NMR (CD_3OD): δ 0.62 [s, 3H, ^2J(Pt−H) = 64 Hz, PtMe]; 1.08 [s, 3H, ^2J(Pt−H) = 70 Hz, PtMe]; 1.51−2.12 [br m, 6H, Cy]; 2.46 [m, 2H, Cy]; 4.01 [br s, 1H]; 4.60 [m, 1H]; 5.34 [s, 1H, ^2J(Pt−H) = 70 Hz, PtCHR−NH]; 7.93 [m, 1H]; 8.01 [m, 1H]; 8.29−8.43 [m, 2H]; 8.45 [br m, 1H]; 8.61 [m, 1H]; 8.84 [m, 1H]; 8.90 [m, 1H]; 9.50 [d, 1H, ^3J(Pt−H) = 33 Hz, PtMe]. IR (Nujol, cm^{-1}): 729 (m), 784 (m), 968 (w), 998 (w), 1033 (w), 1083 (w), 1173 (w), 1247 (w), 1312 (w), 1606 (m), 1636 (m), 2449 (m), 2598 (m), 2658 (m), 3376 (br s).

***R,S/S,R*-[PtClMe$_2${*cis*-1,2-C$_6$H$_{10}$(*N*=CH-2-C$_9$H$_6$*N*)(NH$_2$*C*H-2-C$_9$H$_6$NH)}][Cl]$_2$ (14)** was similarly prepared from complex **4**. Yield: 40%. Anal. Calcd for $C_{28}H_{39}N_4O_3PtCl_3$: C, 43.1; H, 5.0; N, 7.2. Found: C, 43.0; H, 4.6; N, 7.3. ^{1}H NMR (CD_3OD): δ 0.83 [s, 3H, ^2J(Pt−H) = 66 Hz, PtMe]; 0.98 [s, 3H, ^2J(Pt−H) = 68 Hz, PtMe]; 1.60−2.08 [m, 6H, Cy]; 2.49 [m, 1H, Cy]; 2.62 [m, 1H, Cy]; 3.99 [br s, 1H, NCH]; 4.75 [m, 1H, NCH]; 5.54 [s, 1H, ^2J(Pt−H) = 68 Hz, PtCHR−NH]; 7.83 [m, 2H]; 8.03 [m, 1H]; 8.15−8.46 [m, 7H]; 8.92 [d, 1H]; 9.19 [d, 1H]; 9.78 [s, 1H, ^3J(Pt−H) = 35 Hz, N=CH].

***R,S/S,R*-[Pt(O$_2$CCF$_3$)Me$_2${*cis*-1,2-C$_6$H$_{10}$(*N*=CH-2-C$_5$H$_4$*N*)-(NH$_2$-*C*H-2-C$_5$H$_4$NH)}][CF$_3$CO$_2$]$_2$ (15).** To a stirred solution of **4** (0.052 g, 0.10 mmol) in CH_2Cl_2 (10 mL) was added an excess of CF_3CO_2H (38.7 μL, 0.50 mmol), turning the red solution yellow. After 30 min the solvent was evaporated to give an orange-yellow solid. The product was dried extensively under vacuum pressure to remove excess CF_3CO_2H. Recovered yield: 0.048 g (80%). Anal. Calcd for $C_{26}H_{29}N_4PtO_6F_9$: C, 36.3; H, 3.4; N, 6.5. Found: C, 35.8; H, 3.2; N, 6.1. The complex was also prepared in situ by addition of a large excess of CF_3CO_2H to a CD_2Cl_2 solution of **4**. ^{1}H NMR (CD_2Cl_2): δ 0.68 [s, 3H, ^2J(Pt−H) = 62 Hz, PtMe]; 1.14 [s, 3H, ^2J(Pt−H) = 72 Hz, PtMe]; 1.32−1.88 [br m, 4H, Cy]; 2.01 [m, 2H, Cy]; 2.40 [m, 2H, Cy]; 3.39 [br s, 1H, NCH]; 4.46 [m, 1H, NCH]; 5.50 [s, 1H, ^2J(Pt−H) = 63 Hz, PtCHR−NH]; 7.87 [m, 2H]; 8.01 [br d, 1H]; 8.20 [m, 1H]; 8.28 [m, 1H]; 8.44 [m, 1H]; 8.76 [m, 2H]; 9.30 [s, 1H, ^3J(Pt−H) = 32 Hz, N=CH]. ^{13}C NMR (CD_2Cl_2): δ −7.0 [^1J(Pt−C) = 668 Hz, PtMe]; −2.8 [^1J(Pt−C) = 660 Hz, PtMe]; 18.7 [CH_2]; 24.5 [CH_2]; 29.4 [CH_2]; 30.6 [CH_2]; 40.0 [^1J(Pt−C) = 732 Hz, PtCHR−NH]; 59.5 [NCH]; 65.1 [NCH]; 124.6 [^3J(Pt−C) = 9 Hz, CH]; 126.4 [^3J(Pt−C) = 17 Hz, CH]; 129.3 [^3J(Pt−C) = 14 Hz, CH]; 130.2 [^3J(Pt−C) = 9 Hz, CH]; 141.3 [CH]; 141.5 [CH]; 144.2 [CH]; 148.1 [^2J(Pt−C) = 16 Hz, CH]; 154.5 [C]; 156.8 [C]; 169.1 [N=CH]. ^{19}F NMR (CD_2Cl_2): δ −76.1 (s), −76.3 (s).

Table 7. Crystallographic Details for Complexes 5, 6, 8, 12, and 13

	5	6	8	12	13
formula	$C_{20}H_{29}ClN_4OPt$	$C_{20}H_{33}ClN_4O_3Pt$	$C_{23}H_{29}Cl_2F_3N_4O_2Pt$	$C_{30.50}H_{32}ClF_3N_4O_2Pt$	$C_{20}H_{31}Cl_3N_4OPt$
fw	572.01	602.00	716.49	774.14	644.93
temp, K	200(2)	292(2)	293(2)	292(2)	293(2)
wavelength, λ	0.71073	0.710 73	0.710 73	0.710 73	0.710 73
cryst syst	monoclinic	orthorhombic	monoclinic	triclinic	monoclinic
space group	$P2_1/n$	$Pbca$	$P2_1/c$	$P\bar{1}$	$P2_1/c$
a, Å	9.6554(7)	10.45500(10)	12.1563(3)	9.7031(2)	12.5685(1)
b, Å	13.7421(10)	17.3762(4)	17.2318(7)	11.7108(3)	14.3515(2)
c, Å	16.2126(9)	25.0232(6)	13.2224(4)	14.8947(4)	14.1590(1)
α, deg				99.4890(10)	
β, deg	101.382(4)		106.158(2)	102.3460(13)	100.031(1)
γ, deg				91.5210(13)	
V, Å^3	2108.9(2)	4545.92(16)	2660.35(15)	1627.38(7)	2514.19
Z	4	8	4	2	4
d(calcd), Mg/m^3	1.802	1.759	1.789	1.580	1.703
abs coeff, mm^{-1}	6.797	6.318	5.524	4.442	5.916
F(000)	1120	2352	1400	762	1264
no. of rflns	21 869	29 900	26 120	16 599	14 011
no. of indep rflns	3748	4997	6074	6645	5096
no. of data/restraints/params	3748/2/252	4997/0/262	6074/0/345	6645/2/390	5096/0/272
GOF on F^2	0.862	1.040	0.961	1.067	1.153
$R(I > 2\sigma(I))$	R1 = 0.0373, wR2 = 0.0494	R1 = 0.0409, wR2 = 0.1091	R1 = 0.0322, wR2 = 0.0555	R1 = 0.0321, wR2 = 0.0873	R1 = 0.0271, wR2 = 0.0714
R(all data)	R1 = 0.0949, wR2 = 0.0580	R1 = 0.0485, wR2 = 0.1159	R1 = 0.0699, wR2 = 0.0623	R1 = 0.0346, wR2 = 0.0897	R1 = 0.0327, wR2 = 0.0746

***R,S/S,R*-[Pt(O_2CCF_3)Me_2\{*cis*-1,2-C_6H_{10}(*N*=CH-2-C_9H_6*N*)-(NH_2-*C*H-2-C_9H_6NH)\}][CF_3CO_2]$_2$ (16)** was similarly prepared from complex **4**. Yield: 76%. Anal. Calcd for $C_{34}H_{33}N_4PtO_6F_9$: C, 42.6; H, 3.4; N, 5.8. Found: C, 42.4; H, 3.3; N, 5.8. ^{1}H NMR (CD_2Cl_2): δ 0.98 [s, 3H, ^2J(Pt−H) = 63 Hz, PtMe]; 1.19 [s, 3H, ^2J(Pt−H) = 70 Hz, PtMe]; 1.60−2.50 [m, 8H, Cy]; 4.13 [m, 1H, NCH]; 4.70 [m, 1H, NCH]; 5.62 [s, 1H, ^2J(Pt−H) = 62 Hz, PtCHR−NH]; 7.81−7.91 [m, 2H]; 7.98−8.36 [m, 8H]; 8.80 [d, 1H]; 9.40 [d, 1H]; 9.57 [s, 1H, ^3J(Pt−H) = 34 Hz, N=CH]. ^{13}C NMR (CD_2Cl_2): δ −0.6 [^1J(Pt−C) = 635 Hz, PtMe]; 3.9 [^1J(Pt−C) = 608 Hz, PtMe]; 18.5 [CH_2]; 23.9 [CH_2]; 28.8 [CH_2]; 30.2 [CH_2]; 36.9 [^1J(Pt−C) = 779 Hz, PtCHR−NH]; 61.6 [^2J(Pt−C) = 10 Hz, NCH]; 66.8 [NCH]; 120.3 [CH]; 125.2 [^3J(Pt−C) = 12 Hz, CH]; 126.1 [CH]; 128.6 [C]; 129.9 [CH]; 130.0 [CH]; 131.3 [CH]; 131.9 [CH]; 134.4 [CH]; 137.6 [CH]; 138.6 [C]; 143.7 [CH]; 146.8 [^2J(Pt−C) = ca. 12 Hz, C]; 147.9 [CH]; 149.9 [C]; 155.3 [^2J(Pt−C) = ca. 8 Hz, C]; 155.9 [^2J(Pt−C) = ca. 22 Hz, C]; 172.3 [^2J(Pt−C) = ca. 5 Hz, N=CH]. ^{19}F NMR (CD_2Cl_2): δ −75.8 (s); −76.3 (s).

X-ray Structure Determinations. Data were collected using a Nonius Kappa-CCD diffractometer using COLLECT (Nonius, 1998) software. The unit cell parameters were calculated and refined from the full data set. Crystal cell refinement and data reduction were carried out using the Nonius DENZO package. The data were scaled using SCALEPACK (Nonius, 1998), and no other absorption corrections were applied. The SHELXTL 5.1 (G. M. Sheldrick, Madison, WI) program package was used to solve the structure by direct methods, followed by refinement by successive difference Fourier analyses. The crystal data and refinement parameters are listed in Table 7.

Crystals of **5**·H_2O were grown by slow diffusion of pentane into a dichloromethane solution at dry ice temperature. An orange crystal was mounted on a glass fiber. All non-hydrogen atoms were refined with anisotropic thermal parameters. The hydrogen atoms were calculated geometrically and were riding on their respective carbon atoms. One of the methyl groups showed slight disorder; the CH_3 moiety was modeled as six half-occupancy hydrogens rotated by 60°. The water molecule was refined well with the hydrogens fixed at 0.84 Å from the oxygen. The water molecule formed a weak bridge between adjacent platinum molecules. The largest residual electron density peak (1.333 e/Å^3) was associated with the platinum atom.

Crystals of **6**·3H_2O were grown from a saturated methylene chloride solution at dry-ice temperature. An orange crystal was mounted in a capillary. Three molecules of water were found in the asymmetric unit. These were modeled by an anisotropic oxygen, as the hydrogen atoms of the water molecules were not found. The largest residual electron density peak (1.111 e/Å^3) was associated with the platinum atom.

Crystals of **8**·CH_2Cl_2 were grown from slow diffusion of pentane into a dichloromethane solution. An orange crystal was mounted on a glass fiber. Data were collected at 20 °C. The anion showed slight disorder; the CF_3 moiety was modeled as two half-occupancy groups rotated by 60°. All non-hydrogen atoms were refined with anisotropic thermal parameters. The hydrogen atoms were calculated geometrically and were riding on their respective carbon atoms. The largest residual electron density peak (0.759 e/Å^3) was associated with one of the platinum methyl groups.

Crystals of **12**·0.5CH_2Cl_2 were grown from slow diffusion of pentane into a methylene chloride solution. A red block was mounted on a glass fiber. Data were collected at room temperature. The hydrogen atoms were calculated geometrically and were either riding on their respective carbon atoms or riding as rigid groups in the case of the methyl ligands. The methylene chloride of solvation had an occupation factor of 0.5, and the C−Cl distances were fixed at 1.65 Å. Examination of the environment adjacent to O(46) showed a close contact (2.295 Å) to the nitrogen hydrogen (H(19A)).

A yellow crystal of **13**·H_2O was mounted in a capillary. The water molecule was located in a difference map and was disordered over four positions. All heavy atoms were refined anisotropically.

Acknowledgment. We thank the NSERC of Canada for financial support and for the award of a Postgraduate Scholarship to C.R.B.

Supporting Information Available: Tables of X-ray data for **5**, **6**, **8**, **12**, and **13**. This material is available free of charge via the Internet at http://pubs.acs.org.

OM0007769